

Basis Choices for Frequency Domain Statistical Independence Tests and Algorithms for Algebraic Relation Extraction *

Juan Shi[†], Wenbo Wang[‡], Wan Zhang[§], Han Bao[†], Sergio Chavez[†], Jingfang Huang^{†¶},
Yichao Wu^{||}, and Kai Zhang[#]

Abstract. In this paper, we explore how different selections of basis functions impact the efficacy of frequency domain techniques in statistical independence tests, and study different algorithms for extracting low-dimensional algebraic relations from dependent data. We examine a range of complete orthonormal bases functions including the Legendre polynomials, Fourier series, Walsh functions, and standard and nonstandard Haar wavelet bases. We utilize fast transformation algorithms to efficiently transform physical domain data to frequency domain coefficients. The main focuses of this paper are the effectiveness of different basis selections in detecting data dependency using frequency domain data, e.g., whether varying basis choices significantly influence statistical power loss for small data with large noise; and on the stability of different optimization formulations for finding proper algebraic relations when data are dependent. We present numerical results to demonstrate the effectiveness of frequency domain-based statistical analysis methods and provide guidance for selecting the proper basis and algorithm to detect a particular type of relations.

Key words. bump hunting, fast transformation algorithms, frequency domain analysis, harmonic analysis, independence test, orthogonal polynomials, wavelets

MSC codes. 42C10, 62E17, 62G10, 62H10, 65T50, 65T60

1. Introduction. Spectral or frequency domain analysis is a well-developed technique in science and engineering. Classical results include the Laplace transform, Fourier transform and Fourier series, orthogonal polynomials, and wavelet analysis. Instead of function values (physical domain data), the frequency domain technique studies the relations of expansion coefficients (frequency domain data) which may show simpler structures when compared with their physical domain counterparts. For example, convolutions in the physical domain become simple products in the frequency domain, and physical domain differential equation models become algebraic relations for the expansion coefficients in the frequency domain.

In this paper, we study how different choices of basis functions impact the numerical properties of the frequency domain techniques when generalized to statistical independence tests. For a given paired data set $\{(x_n, y_n)\}_{n=1}^N$ sampled from an underlying distribution, where both x_n and y_n may be scalar random variables, vectors, or tensors, the physical domain data

*Submitted to the editors DATE.

[†]Department of Mathematics, University of North Carolina at Chapel Hill, Chapel Hill, NC (juans@live.unc.edu, sergio@unc.edu, huang@email.unc.edu).

[‡]Department of Biostatistics, University of North Carolina at Chapel Hill, Chapel Hill, NC (wenbo@live.unc.edu).

[§]Center for Forecasting Science, Academy of Mathematics and System Science, Chinese Academy of Sciences, Beijing, China (wanzhang@amss.ac.cn).

[¶]Corresponding Author.

^{||}Department of Mathematics, Statistics and Computer Science, University of Illinois at Chicago, Chicago, IL (yichaowu@uic.edu).

[#]Department of Statistics and Operations Research, University of North Carolina at Chapel Hill, Chapel Hill, NC (zhangk@email.unc.edu).

set $\{(x_n, y_n)\}_{n=1}^N$ can be transformed into new frequency domain data which can be utilized to address one of the most fundamental questions in statistics: whether the variables x and y are dependent. Once the variables are discovered to be dependent, the frequency domain data can also be utilized to identify the structure of the dependence or relation.

The concepts of dependence and correlations of random data sets have been studied for over a century. Classical parametric dependence tests include Pearson’s correlation test, χ^2 -test, and t-test. When the dependence satisfies a linear relationship, linear regression is a well-developed technique with extensive applications in physical, biomedical, financial, and social sciences. More recent developments include [5, 7, 10, 11, 12, 16, 17, 25, 26, 27, 29, 33, 34, 35, 36, 38, 39, 43, 46, 52, 53, 56, 63, 65, 66], with several notable contributions from computer scientists [37, 48, 49, 50], reflecting the general attention to this problem from the broader Data Science community. Once the variables are determined dependent, it is a common practice to find any low-dimensional or compressible features in the data. A partial list of existing compressible features and their extraction strategies include the “bump” function $y = f(x) = \mathbb{E}(Y|X = x)$ and bump hunting techniques [22], approximation with smooth functions in generalized additive models [31], projection pursuit regression [23], optimization in variational inference [8], minimum average variance estimation (MAVE) [62], sliced inverse regression [41], and kernel density reduction and estimation [24, 51].

The ideas of frequency domain statistical data analysis have been studied in the past, some recent results include the binary expansion testing (BET) [63], binary expansion adaptive symmetry test (BEAST) [64], and binary expansion linear effect (BELIEF) [9]. Both these techniques transform the physical domain data nonlinearly to a set of frequency domain coefficients of the Walsh (Walsh-Hadamard) expansion of the probability density function. The independence test is then performed on the expansion coefficients to extract interesting statistical features. In this paper, in addition to the Walsh basis, we study different basis choices for frequency domain statistical independence tests, including the Legendre polynomials, Fourier series, and standard and nonstandard Haar wavelet bases. We introduce fast transformation algorithms and present the mathematically equivalent formulations for different statistical signatures in the transformed frequency domain. When the data follow low-dimensional dependence relations, we study how to stably find the “bump” function $y = f(x) = \mathbb{E}(Y|X = x)$ in the frequency domain. By studying a simplified yet representative class of separable relations in the form of $H(x) = G(y)$, we also present some numerical algorithms and address their stability issues for finding more general algebraic relations. The contributions of this paper include comparisons of different choices of basis functions for frequency domain statistical independence tests, fast transformation algorithms, and more stable bump hunting algorithms in the frequency domain. Compared with existing physical domain techniques, the frequency domain statistical data analysis framework may provide new strategies for more efficient statistical testing and compressible feature extraction with improved statistical power and numerical stability.

This paper presents the basic ideas of the frequency domain statistical data analysis from an *applied analysis perspective*, and is organized as follows. In [section 2](#), we briefly discuss classical frequency domain analysis concepts and demonstrate how to “sample” the expansion coefficients and higher order moments efficiently using fast transformation algorithms. In [subsection 3.1](#), we present the frequency domain statistical signatures of two indepen-

dent scalar X and Y random variables and present two numerical estimators for statistical independence tests. In [subsection 3.2](#), we show how to stably find the “bump” function $y = f(x) = \mathbb{E}(Y|X = x)$ using frequency domain data. We then present a canonical-correlation analysis (CCA) algorithm and its equivalent frequency domain singular value decomposition algorithm for identifying more general separable low-dimensional structures in the form of $H(x) = G(y)$. In [section 4](#), numerical results are presented to validate our analysis and to demonstrate the algorithms’ performance and numerical stability. We finally summarize our results and discuss a few ongoing research efforts in [section 5](#).

2. Transform Physical Domain Data to Frequency Domain. Consider a single variable function $f(x)$, $-1 \leq x \leq 1$, the classical spectral/frequency domain analysis considers its expansion in the form of

$$(2.1) \quad f(x) = \sum_{i=0}^{\infty} c_i \phi_i(x)$$

where $\{\phi_i(x)\}_{i=0}^{\infty}$ is a complete orthonormal basis set. Instead of studying the physical domain function values $f(x)$ directly, the frequency domain technique studies the expansion coefficients c_i . The data set $\{c_i\}_{i=0}^{\infty}$ is referred to as the spectral or frequency domain data. Clearly, the mapping from x to $\phi_i(x)$ is in general nonlinear.

2.1. Choice of Basis in One Dimension. For a single-variable function, the choice of the basis set $\{\phi_i(x)\}$ is a well-studied topic in applied analysis. Each basis set is related to an inner product space. In this paper, we focus on four commonly used basis sets in one dimension: the Legendre polynomials, Fourier series, Walsh functions, and Haar wavelet basis.

Legendre Polynomials: When the inner product is defined as $\langle f, g \rangle = \int_{-1}^1 f(x)g(x)dx$, an orthogonal polynomial basis set $\{P_k(x)\}_{k=0}^{\infty}$ can be constructed using the Gram-Schmidt process. The first four of these Legendre polynomials are given by $P_0(x) = 1$, $P_1(x) = x$, $P_2(x) = \frac{1}{2}(3x^2 - 1)$, and $P_3(x) = \frac{1}{2}(5x^3 - 3x)$. Similar to the properties of other orthogonal polynomial basis sets, the Legendre polynomials have a generating function

$$\frac{1}{\sqrt{1 - 2xt + t^2}} = \sum_{n=0}^{\infty} P_n(x)t^n$$

and a three-term recurrence relation

$$(n+1)P_{n+1}(x) = (2n+1)xP_n(x) - nP_{n-1}(x),$$

which is often applied to accelerate the evaluation of the polynomial expansions. Legendre polynomials are solutions to Legendre’s differential equation

$$(1 - x^2)P_n''(x) - 2xP_n'(x) + n(n+1)P_n(x) = 0.$$

Interested readers are referred to [\[1, 42\]](#) for a complete list of the properties of the Legendre (and other orthogonal) polynomials. In this paper, we use orthonormal basis sets for all expansions. Instead of the standard Legendre polynomials which satisfy

$$\int_{-1}^1 P_M(x)P_n(x)dx = \frac{2}{2n+1}\delta_{nm},$$

the normalized orthonormal Legendre polynomial basis is given by $L_n(x) = \sqrt{\frac{2n+1}{2}} P_n(x)$.

Fourier Series: Fourier series is a useful tool to study smooth periodic functions. Using the complex representation, the Fourier series of a function $f(x)$ which is periodic with a fundamental period of 2 is

$$f(x) = \sum_{k=-\infty}^{\infty} c_k e^{ik\pi x}$$

where $i = \sqrt{-1}$ and $c_k = \frac{1}{2} \int_{-1}^1 f(x) e^{-ik\pi x} dx$. Compared with orthogonal polynomials, the properties of the Fourier series are much simpler: The generating function of the Fourier series is the (periodic) Dirac Delta function, the three-term recurrence relation is simply $e^{i(j+1)\pi x} = e^{ij\pi x} e^{i\pi x}$, and the basis $e^{ij\pi x}$ is the solution of the simple differential equation

$$u_n''(x) + (j\pi)^2 u(x) = 0.$$

In this paper, similar to the Legendre basis $L_n(x)$, we use the normalized complex form Fourier basis functions $\phi_n(x) = \frac{1}{\sqrt{2}} e^{in\pi x}$.

Walsh Functions: Wavelet transforms are commonly used in image and signal analysis. One particular wavelet basis set is the Walsh functions [6, 60] which consist of trains of square pulses (with the allowed states being -1 and 1) such that transitions may only occur at fixed intervals of a unit time step. The initial state is always $+1$, and the functions satisfy the orthogonality relations and they all have norm one. In particular, the 2^n Walsh functions of order n are given by the rows of the Hadamard matrix H_{2^n} when arranged in so-called “sequency” order [58]. The Walsh functions are often considered as the discrete version of the *sine* and *cosine* functions in a Fourier series expansion. The wavelet basis may perform better when the underlying function has discontinuities as discussed in [55], where the author compared the performance of wavelet expansions with Fourier series for different applications.

Haar Wavelets: Another choice of wavelet basis is the Haar wavelet [30] consisting of a sequence of square-shaped functions constructed using the scaling function $s(t)$ and mother wavelet function $m(t)$ given by

$$s(x) = \begin{cases} 1 & 0 \leq x < 1 \\ 0 & \text{otherwise} \end{cases}$$

$$m(x) = \begin{cases} 1 & 0 \leq x < \frac{1}{2} \\ -1 & \frac{1}{2} \leq x < 1 \\ 0 & \text{otherwise.} \end{cases}$$

The non-normalized basis functions at level i are given by the formula $\psi_{i,j}(t) = m(2^i t - j)$ where $j = 0, 1, \dots, 2^i - 1$. Similar to the Legendre and Fourier basis functions, we also normalize the Haar basis functions using $H_0(t) = s(t)$ and $H_k(t) = 2^i \psi_{i,j}(t)$ so that the rescaled Haar basis functions satisfy $\|H_k(x)\|_2 = 1$ for all k values. An interesting feature of the Haar basis is the “local” (sparse) property of the higher-level basis functions, i.e., the basis is only nonzero in a small region for large k values.

2.2. Choice of Basis in Higher Dimensions. The single variable frequency domain analysis can be easily extended to study multi-variable functions. Using the tensor/Kronecker product, higher-dimensional basis sets can be constructed using one-dimensional basis functions. For a function $f(x, y)$ with two variables, the basis functions are $\{\phi_i(x)\psi_j(y)\}_{i,j=0}^{\infty}$ where $\{\phi_i(x)\}$ and $\{\psi_j(y)\}$ are the (not necessarily the same) one-dimensional basis sets for the x - and y -variables, respectively. The function expansion is then given by

$$f(x, y) = \sum_{i,j} c_{i,j} \phi_i(x) \psi_j(y).$$

Note that non-tensor-product bases can also be used and a more general expansion is then given by

$$f(x, y) = \sum_k c_k \Phi_k(x, y)$$

where $\{\Phi_k(x, y)\}_{k=0}^{\infty}$ is an arbitrary two-dimensional orthonormal basis.

An interesting non-tensor-product wavelet basis is the nonstandard Haar wavelet basis [54] constructed using the one-dimensional functions $s_{i,j}(t) = s(2^i t - j)$ and $m_{i,j}(t) = m(2^i t - j)$ with sparser and more local properties. In Fig. 2.1, we plot the first 2 levels of nonstandard Haar basis functions in two dimensions. In the plot, the “+” and “−” signs represent a positive constant $+c$ and a negative constant $-c$, respectively. The constant c is chosen so that the nonstandard Haar wavelet basis functions are normalized. At deeper levels, the basis functions are zero in most regions and are hence “sparse” and “local”. Note that the nonstandard Haar basis is naturally associated with an adaptive hierarchical tree structure, which allows faster computation of the expansion coefficients. For high-dimensional data located on a low-dimensional manifold, the “sparse” nonstandard Haar wavelet basis is a better choice compared with other “all-grid” tensor-product based basis choices such as the Legendre polynomials, Fourier series, and Walsh functions.

2.3. Transform from Physical Domain to Frequency Domain. We demonstrate the transformation from the physical domain to the frequency domain using two-dimensional data sets. Assume that N sampled data points $\{(x_n, y_n)\}_{n=1}^N$ are located in the square $[a, b]^2$, where $[a, b] = [-1, 1]$ for the Legendre polynomials and Fourier series, and $[a, b] = [0, 1]$ for the Walsh and Haar wavelet bases. We consider the two-dimensional basis set $\{\phi_{k_1}(x)\phi_{k_2}(y)\}_{k_1,k_2=0}^{\infty}$ constructed using the tensor product applied to a general one-dimensional orthonormal basis set $\{\phi_k(x)\}_{k=0}^{\infty}$ for the domain $[a, b]$. We use the same basis set for both x - and y -variables. The generalizations of our results to a two-dimensional basis set constructed using the tensor product of two different one-dimensional basis sets and to a non-tensor-product orthonormal basis are straightforward. We skip the details in this paper.

Assume that the frequency domain representation of the underlying physical domain probability density function $f(x, y)$ for the data points $\{(x_n, y_n)\}_{n=1}^N$ is given by

$$f(x, y) = \sum_{k_1, k_2} c_{k_1, k_2} \phi_{k_1}(x) \phi_{k_2}(y).$$

For fixed k_1 and k_2 , by applying the orthogonality properties of the basis functions, we have the following theorem which states that each datum $\phi_{k_1}(x_n)\phi_{k_2}(y_n)$ can be considered as a “sample” of the expansion coefficient c_{k_1, k_2} .

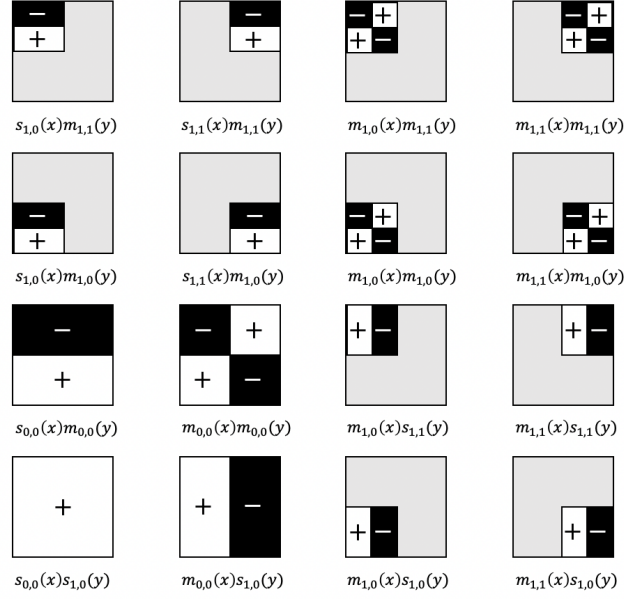


Figure 2.1: The nonstandard construction of a two-dimensional Haar wavelet basis

Theorem 2.1. $\mathbb{E}[\phi_{k_1}(X)\phi_{k_2}(Y)] = \int \int \phi_{k_1}(x)\phi_{k_2}(y)f(x,y)dxdy = c_{k_1,k_2}$.

We introduce the following definition.

Definition 2.2. For each pair of physical domain data (x_n, y_n) , the (nonlinearly) transformed data sets $\{\phi_{k_1}(x_n)\phi_{k_2}(y_n)\}_{n=1}^N$ for $k_1, k_2 = 0, \dots, \infty$ are called the frequency domain data sets.

Given N sample points, using the frequency domain data sets $\{\phi_{k_1}(x_n)\phi_{k_2}(y_n)\}_{n=1}^N$ and Monte Carlo integration, the numerical estimates of the frequency domain coefficients are

$$(2.2) \quad \hat{c}_{k_1,k_2} = \frac{1}{N} \sum_{n=1}^N \phi_{k_1}(x_n)\phi_{k_2}(y_n).$$

The frequency domain coefficient matrix $C = [c_{k_1,k_2}]$ can be approximated by $\hat{C} = [\hat{c}_{k_1,k_2}]$.

When a tensor product is applied to construct a two-dimensional orthonormal basis, we can also study the statistical properties of the special sets of frequency domain data $\{\phi_{k_1}(x_n)\}_{n=1}^N$ and $\{\phi_{k_2}(y_n)\}_{n=1}^N$. Clearly,

$$\mathbb{E}\left[\begin{bmatrix} \phi_0(X) \\ \phi_1(X) \\ \vdots \\ \phi_K(X) \end{bmatrix}\right] = \begin{bmatrix} c_{0,0} \\ c_{1,0} \\ \vdots \\ c_{K,0} \end{bmatrix} \quad \text{and} \quad \mathbb{E}\left[\begin{bmatrix} \phi_0(Y) \\ \phi_1(Y) \\ \vdots \\ \phi_K(Y) \end{bmatrix}\right] = \begin{bmatrix} c_{0,0} \\ c_{0,1} \\ \vdots \\ c_{0,K} \end{bmatrix}.$$

Following classical statistical analysis theory, we define the variance matrices of $\{\phi_{k_1}(x_n)\}_{n=1}^N$ and $\{\phi_{k_2}(y_n)\}_{n=1}^N$ as

$$\begin{aligned}\Sigma_{XX} &= \mathbb{E} \left[\left(\begin{bmatrix} \phi_0(X) \\ \phi_1(X) \\ \vdots \\ \phi_K(X) \end{bmatrix} - \begin{bmatrix} c_{0,0} \\ c_{1,0} \\ \vdots \\ c_{K,0} \end{bmatrix} \right) \left(\begin{bmatrix} \phi_0(X) \\ \phi_1(X) \\ \vdots \\ \phi_K(X) \end{bmatrix} - \begin{bmatrix} c_{0,0} \\ c_{1,0} \\ \vdots \\ c_{K,0} \end{bmatrix} \right)^T \right] \\ &= \mathbb{E}[\phi_k(X)\phi_m(X)] - \begin{bmatrix} c_{0,0} \\ c_{1,0} \\ \vdots \\ c_{K,0} \end{bmatrix} [c_{0,0}, c_{1,0}, \dots, c_{K,0}], \\ \Sigma_{YY} &= \mathbb{E} \left[\left(\begin{bmatrix} \phi_0(Y) \\ \phi_1(Y) \\ \vdots \\ \phi_K(Y) \end{bmatrix} - \begin{bmatrix} c_{0,0} \\ c_{0,1} \\ \vdots \\ c_{0,K} \end{bmatrix} \right) \left(\begin{bmatrix} \phi_0(Y) \\ \phi_1(Y) \\ \vdots \\ \phi_K(Y) \end{bmatrix} - \begin{bmatrix} c_{0,0} \\ c_{0,1} \\ \vdots \\ c_{0,K} \end{bmatrix} \right)^T \right] \\ &= \mathbb{E}[\phi_k(Y)\phi_m(Y)] - \begin{bmatrix} c_{0,0} \\ c_{0,1} \\ \vdots \\ c_{0,K} \end{bmatrix} [c_{0,0}, c_{0,1}, \dots, c_{0,K}].\end{aligned}$$

As will be explained in Sec. 3, we can study the relations between the physical domain x - and y -variables using the frequency domain covariance matrix of $\{\phi_{k_1}(x_n)\}_{n=1}^N$ and $\{\phi_{k_2}(y_n)\}_{n=1}^N$ defined as

$$\begin{aligned}\Sigma_{XY} &= \mathbb{E} \left[\left(\begin{bmatrix} \phi_0(X) \\ \phi_1(X) \\ \vdots \\ \phi_K(X) \end{bmatrix} - \begin{bmatrix} c_{0,0} \\ c_{1,0} \\ \vdots \\ c_{K,0} \end{bmatrix} \right) \left(\begin{bmatrix} \phi_0(Y) \\ \phi_1(Y) \\ \vdots \\ \phi_K(Y) \end{bmatrix} - \begin{bmatrix} c_{0,0} \\ c_{0,1} \\ \vdots \\ c_{0,K} \end{bmatrix} \right)^T \right] \\ &= \mathbb{E}[\phi_k(X)\phi_m(Y)] - \begin{bmatrix} c_{0,0} \\ c_{1,0} \\ \vdots \\ c_{K,0} \end{bmatrix} [c_{0,0}, c_{0,1}, \dots, c_{0,K}].\end{aligned}$$

Note that Σ_{XY} is the frequency domain coefficient matrix $C = [c_{k_1, k_2}]$ minus a rank one perturbation matrix. As we always choose $\phi_0(x)$ to be the constant function and perform the copula transformation, the first column and first row of the matrices Σ_{XX} , Σ_{YY} , and Σ_{XY} are therefore always zero except for the first entry,

$$\Sigma_{XX} = \begin{bmatrix} 1 & 0 & \dots & 0 \\ 0 & & & \\ \vdots & \tilde{\Sigma}_{XX} & & \\ 0 & & & \end{bmatrix}, \quad \Sigma_{YY} = \begin{bmatrix} 1 & 0 & \dots & 0 \\ 0 & & & \\ \vdots & \tilde{\Sigma}_{YY} & & \\ 0 & & & \end{bmatrix}, \quad \Sigma_{XY} = \begin{bmatrix} 1 & 0 & \dots & 0 \\ 0 & & & \\ \vdots & \tilde{\Sigma}_{XY} & & \\ 0 & & & \end{bmatrix}.$$

We therefore only need to focus on $\tilde{\Sigma}_{XX}$, $\tilde{\Sigma}_{YY}$, and $\tilde{\Sigma}_{XY}$. Finally, we define the variance of the frequency domain data $\phi_{k_1}(x)\phi_{k_2}(y)$ as

$$\text{var}[\phi_{k_1}(X)\phi_{k_2}(Y)] = \mathbb{E}[(\phi_{k_1}(X)\phi_{k_2}(Y) - c_{k_1,k_2})^2] = \mathbb{E}[(\phi_{k_1}(X)\phi_{k_2}(Y))^2] - c_{k_1,k_2}^2.$$

Higher order moments of the frequency domain data can also be computed which may carry interesting information on the statistical properties of the physical domain data.

Comment: For non-tensor-product bases, e.g., the nonstandard Haar wavelet basis functions, the matrices $\tilde{\Sigma}_{XX}$, $\tilde{\Sigma}_{YY}$, and $\tilde{\Sigma}_{XY}$ are unfortunately not defined. However, it is still possible to define the expectations and higher order moments of the frequency domain data $\{\Phi_k(x_n, y_n)\}$ for $n = 1, \dots, N$ and $k = 0, \dots, \infty$.

One of the main contributions of this paper is a more systematic study of the statistical properties of the physical domain data (x_n, y_n) using the transformed frequency domain data including the (numerically computed random) **frequency domain coefficient matrix** $\hat{C}_{(K+1) \times (K+1)}$, **variance matrices** $\tilde{\Sigma}_{XX}$, $\tilde{\Sigma}_{YY}$, $\tilde{\Sigma}_{XY}$, $\text{var}[\phi_{k_1}(X)\phi_{k_2}(Y)]$, and higher order moments. Our current study focuses on the low-frequency domain information, where the frequency domain expansion is truncated after the first K terms with $K \leq c \cdot \sqrt{N}$, $c < 1$. Intuitively, accurately capturing all the high-frequency coefficients \hat{c}_{k_1,k_2} would require enough sampling points in one wavelength for each variable. However, it is still possible to get certain high-frequency information when the information is sufficient in certain perspectives (e.g., physical data are dense enough in a small spatial region). This paper studies how to extract statistical information from the physical and frequency domain data under different scenarios.

2.4. Fast Transformation Algorithms. The coefficient and variance matrices \hat{C} , $\tilde{\Sigma}_{XX}$, $\tilde{\Sigma}_{YY}$, $\tilde{\Sigma}_{XY}$, and $\text{var}[\phi_{k_1}(X)\phi_{k_2}(Y)]$ can be efficiently computed using fast transformation algorithms. Using the Fourier basis as an example, we demonstrate how to efficiently compute all the entries in the coefficient matrix \hat{C}

$$\hat{c}_{k_1,k_2} = \frac{1}{N} \sum_{n=1}^N e^{ik_1\pi x_n} e^{ik_2\pi y_n}$$

for $k_1, k_2 = -K, \dots, K$. As the data points (x_n, y_n) are in general not uniformly distributed, and evaluating the summation directly would require $O(NK^2)$ operations. In two dimensions, when $K \sim O(\sqrt{N})$, the total amount of work in a direct method is approximately $O(N^2)$. Following the notation in [28], we notice that the summation for computing \hat{c}_{k_1,k_2} is a special case of the Type I nonuniform discrete Fourier transform (see Eq. (1) in [28]) where the weight for each data pair is 1, therefore existing nonuniform fast Fourier transform (NuFFT) algorithms can be applied to reduce the total amount of work from $O(N^2)$ to $O(N \log N)$ [18, 19, 28, 40, 47]. The NuFFT algorithm is based on the $O(N \log N)$ Fast Fourier Transform (FFT) algorithm for uniformly distributed points [14]. Interested readers are referred to [32] for the history of the development of FFT algorithms.

For other basis choices, existing uniform fast Legendre transform (FLT) packages are at least 5 ~ 10 times slower than the well-developed (and hardware-implemented) uniform FFT solvers; both uniform and non-uniform fast Walsh-Hadamard transform (FWHT) and fast Haar transform (FHT) are available to accelerate the computation of the random frequency

domain coefficient matrix \hat{C} . When the nonstandard Haar wavelet basis is used, because of the sparsity and locality in the basis functions and by utilizing the associated hierarchical tree structure, the accelerated computation of the nonstandard Haar wavelet expansion can be asymptotically optimal in efficiency and allows for easy coupling with an adaptive tree structure when data are located on low-dimensional manifolds. This feature makes the nonstandard Haar basis appealing for very high-dimensional data sets which are located on a low-dimensional manifold. In engineering applications, the Walsh and Haar wavelet bases may show better performance when the underlying function has discontinuities as discussed in [55]. We have implemented and tested some of these fast transformation algorithms. Our numerical results show that the fast transformations from the physical domain to the frequency domain can be orders of magnitude more efficient, especially for a large number of data points.

3. Frequency Domain Statistical Analysis. We demonstrate how the frequency domain data can be utilized to study the dependence of two scalar random variables X and Y , and when they are dependent, how to find possible low-dimensional structures in the data.

3.1. Independence Test. In the physical domain, two random variables X and Y are independent if and only if their joint distribution function satisfies $f(x, y) = h(x)g(y)$, where $h(x)$ and $g(y)$ are the marginal distribution functions for X and Y , respectively. When a two-variable function $f(x, y)$ is given by the product of two single variable functions $h(x)$ and $g(y)$, we refer to $f(x, y)$ as a **rank-1** function.

In the frequency domain, when using the same set of one-dimensional basis functions $\{\phi_k\}_{k=0}^{\infty}$ with $\phi_0 = \frac{1}{\|1\|}$ (constant function), one can expand $h(x)$ and $g(y)$ as

$$h(x) = \sum_{j=0}^{\infty} h_j \phi_j(x) \text{ and } g(y) = \sum_{k=0}^{\infty} g_k \phi_k(y),$$

respectively. The frequency domain expansion of $f(x, y)$ is then given by

$$f(x, y) = \sum_{j,k=0}^{\infty} c_{j,k} \phi_j(x) \phi_k(y) = \sum_{j,k=0}^{\infty} h_j g_k \phi_j(x) \phi_k(y).$$

Therefore, the coefficients satisfy the relation $c_{j,k} = h_j \cdot g_k$ and the truncated coefficient matrix

$$C_{K \times K} = [h_0, h_1, \dots, h_K]^T [g_0, g_1, \dots, g_K]$$

is a rank-1 matrix. We have the following theorem for the frequency domain data.

Theorem 3.1. *Assume the joint probability distribution function $f(x, y)$ of two random variables X and Y has the frequency domain expansion $f(x, y) = \sum_{j,k=0}^{\infty} c_{j,k} \phi_j(x) \phi_k(y)$. Then X and Y are independent if and only if the expansion coefficient matrix $C = [c_{j,k}]$ is a rank-1 matrix $C = [h_0, h_1, \dots]^T [g_0, g_1, \dots]$.*

Determining whether a random matrix is rank-1 is theoretically possible but numerically more challenging. Therefore, following standard practice in statistical analysis, to study whether Y is dependent on X , one can first apply a “copula” transform to Y so that the transformed Y variable follows a uniform distribution on the interval $[0, 1]$. We can simplify Theorem 3.1 as follows.

Theorem 3.2. Assume the joint probability distribution function $f(x, y)$ of two random variables X and Y has the frequency domain expansion $f(x, y) = \sum_{j,k=0}^{\infty} c_{j,k} \phi_j(x) \phi_k(y)$ and the marginal distribution of Y follows the uniform distribution $U[0, 1]$. Then X and Y are independent if and only if the expansion coefficient matrix $C = [c_{j,k}]$ is a rank-1 matrix $C = [h_0, h_1, h_2, \dots]^T [1, 0, 0, \dots]$. Equivalently, the expansion coefficients $c_{j,k} = 0$ for any $k \neq 0$.

Therefore, after applying the copula transform to y -variable, the task of testing independence becomes that of testing whether the frequency domain data satisfy $c_{j,k} = 0$ for any $k \neq 0$.

When Y and X are independent and after performing the copula transform to Y , we have $\mathbb{E}[\phi_j(X) \phi_k(Y)] = c_{j,k} = 0$ ($k \neq 0$) independent of the marginal distribution of X . However, other statistical properties of $\phi_j(x) \phi_k(y)$ will depend on the marginal distribution of X (e.g., its variance). This dependency implies that for any frequency domain estimator in the statistical independence test, its distribution for the independent case cannot be precomputed as the marginal distribution of X is unknown. It is possible to run a permutation test which permutes either the X , or Y , or both variables [3, 13, 20, 21], and the permuted data sets are used to estimate the distribution function of $\phi_j(x) \phi_k(y)$ for the independent cases. The on-the-fly permutation test is normally very expensive. For optimal numerical stability and efficiency (and simplified notation and discussion), when studying the dependence between two random variables X and Y , we assume that the cumulative distribution function of the physical domain data $\{(x_n, y_n)\}_{n=1}^N$ is a copula and the marginal probability distributions of both variables X and Y are uniform on the interval $[0, 1]$. Introducing a proper orthonormal basis set $\{\phi_k(x)\}_{k=0}^{\infty}$ for the domain $[0, 1]$ with $\phi_0(x) = \frac{1}{\|1\|}$ and constructing the corresponding orthonormal basis for $[0, 1]^2$ using the tensor product, Theorem 3.2 can then be simplified to the following theorem which provides a set of mathematically equivalent frequency domain signatures when X and Y are independent.

Theorem 3.3. Assume $X, Y \sim U[0, 1]$. Then the following statements are equivalent.

1. X and Y are independent.
2. The probability density function is the constant function $f(x, y) = 1$, $0 \leq x, y \leq 1$.
3. $c_{k_1, k_2} = 0$ when $(k_1, k_2) \neq (0, 0)$, where c_{k_1, k_2} are the expansion coefficients of

$$f(x, y) = \sum_{k_1, k_2} c_{k_1, k_2} \phi_{k_1}(x) \phi_{k_2}(y),$$

and $\{\phi_k\}$ is a complete set of orthonormal basis with $\phi_0 = \frac{1}{\|1\|}$.

4. For any $\vec{\alpha}$ and $\vec{\beta}$, define $\psi_1(x) = \sum_k \alpha_k \phi_k(x)$ and $\psi_2(y) = \sum_k \beta_k \phi_k(y)$. Then, the expectation $\mathbb{E}(\psi_1(X) \psi_2(Y)) = \alpha_0 \cdot \beta_0$.
5. $\text{Corr}(\psi_1(X), \psi_2(Y)) = 0$ for any $\vec{\alpha}$ and $\vec{\beta}$.

We also list some necessary (but not sufficient) conditions for X and Y to be independent.

Theorem 3.4. Assume $X, Y \sim U[0, 1]$, X and Y are independent, and $\phi_0(x) = \frac{1}{\|1\|}$, then the frequency domain data have the following features.

1. $\mathbb{E}(\phi_{k_1}^2(x) \phi_{k_2}^2(y)) = 1$.
2. $\text{Corr}(c_{k_1, k_2}, c_{l_1, l_2}) = 0$ if $(k_1, k_2) \neq (l_1, l_2)$.

The first condition in this theorem comes from the fact that all the basis functions are normalized. It also shows the variance of the frequency domain data for the copula-transformed independent data set. The second item shows how the coefficients are correlated. Note that there are many such necessary conditions for the frequency domain data. For example, when $N \gg K$ and $X, Y \sim U[0, 1]$ are independent, then each entry in the frequency domain coefficient matrix C approximately follows a Gaussian distribution. Borrowing results from random matrix theory, the empirical distribution of the eigenvalues of matrix C (Wigner matrix) will converge to certain limiting distributions. Interested readers are referred to [2, 44] and references therein for further results from random matrix theory.

Utilizing the computed frequency domain coefficient matrix $\hat{C} = \{\hat{c}_{k_1, k_2}\}$ and results in Theorem 3.3, we present two algorithms (statistics) for independence testing using the frequency domain data.

Algorithm 1 (Max-FiT): In the first algorithm, we focus on a statistic z defined by $z = \|\hat{C}\|_{\max} = \max_{k_1, k_2} |\hat{c}_{k_1, k_2}|$. When $X, Y \sim U[0, 1]$ are independent and N is large, the new random variable (statistic) z asymptotically follows the generalized extreme value (GEV) distribution [15, 45, 61], a well-studied topic in statistics; its probability density function is available asymptotically and numerically. Algorithm 1 determines whether X and Y are independent by comparing z with the corresponding independent case GEV distribution.

We refer to Algorithm 1 as the Maximal coefficient Frequency-domain independence Test (Max-FiT) and its analysis and properties are very similar to those of the maximal coefficient BET technique discussed in [63], where the Walsh basis is used.

Algorithm 2 (SVD-FiT): In our second algorithm, we use the statistic $z = \|\hat{C}\|_2$, the largest singular value of the computed coefficient matrix \hat{C} , or equivalently, we can study the largest eigenvalue of the Wishart (Laguerre) ensemble of a positive definite matrix $\hat{C}^T \cdot \hat{C}$. The random variable z follows the Tracy-Widom distribution [4, 57, 59] which is also a well-studied topic. The algorithm determines whether X and Y are independent by comparing z with the Tracy-Widom distribution for independent data. We refer to the second algorithm as the Singular Value Decomposition Frequency-domain independence Test (SVD-FiT). This test is closely related to the physical domain χ^2 -test.

In both algorithm implementations, as we have applied the copula transform to each variable, the GEV or Tracy-Widom distributions for the independent case can be pre-constructed to avoid the expensive permutation tests. One can also apply approximate distributions that are asymptotically correct for large sample sizes. Note that in two dimensions, a general data set $\{(x_n, y_n)\}_{n=1}^N$ can be efficiently transformed into a copula data set by applying a quick sort to each of the two random variable sets $\{x_n\}$ and $\{y_n\}$, $n = 1, \dots, N$, respectively. However, for higher-dimensional data, e.g., when x_n is not a scalar but a vector or tensor, “optimally” transforming arbitrary higher-dimensional data into a high-dimensional uniform distribution is still an active research area (e.g., in optimal transport). Therefore, in more general higher-dimensional settings, permutation tests or asymptotic analyses have to be applied to estimate the distributions for the independent cases.

3.2. Finding Low-Dimensional Structures. It is possible and sometimes numerically more convenient (in terms of stability and efficiency) to extract the hidden features of physical do-

main data from the frequency domain coefficient matrix and higher order moments. In this section, we first discuss how to find the “bump” functions defined as $y = H(x) = \mathbb{E}[Y|X = x]$ or $x = G(y) = \mathbb{E}[X|Y = y]$. We then generalize the ideas to find the low-dimensional structures (one dimensional curves in two dimensions) given by the implicit algebraic relation $H(x) = G(y)$ where the data are the perturbed random variables around the curve implicitly given by $H(x) = G(y)$, e.g., the unit circle $x^2 = 1 - y^2$. As we will demonstrate in [section 4](#), finding the separable relation $H(x) = G(y)$ is already numerically challenging and designing a numerically stable algorithm requires better knowledge of many factors, including the underlying noise. Developing numerically stable formulations for more general relations $H(x, y) = 0$ is currently being studied, and results will be reported in a subsequent paper.

3.2.1. Bump Hunting. Bump hunting is a well-studied topic in statistics and applications [\[22\]](#). In bump hunting, for a given set of physical domain data (x_n, y_n) , one searches for a function $H(x)$ (or $G(y)$), such that for any fixed x (or y), $\mathbb{E}[Y - H(X)|X = x] = 0$ (or $\mathbb{E}[X - G(Y)|Y = y] = 0$). Using the joint probability density function $f(x, y)$ and its expansion $f(x, y) = \sum_{i,j} c_{i,j} \phi_i(x) \phi_j(y)$, the bump function satisfies

$$(3.1) \quad \int (y - H(x)) \left(\sum_{i,j} c_{i,j} \phi_i(x) \phi_j(y) \right) dy = 0 \text{ for any } x,$$

or

$$(3.2) \quad \int (x - G(y)) \left(\sum_{i,j} c_{i,j} \phi_i(x) \phi_j(y) \right) dx = 0 \text{ for any } y.$$

Using $H(x)$ in Eq. (3.1) as an example, as

$$\int y \sum_{i,j} c_{i,j} \phi_i(x) \phi_j(y) dy = \int H(x) \sum_{i,j} c_{i,j} \phi_i(x) \phi_j(y) dy$$

and the basis functions are orthonormal with $\phi_0 = \frac{1}{\|1\|}$, we have

$$\sum_i \left(\sum_j c_{i,j} \langle y, \phi_j(y) \rangle \right) \phi_i(x) = H(x) \langle 1, \phi_0(y) \rangle \sum_i c_{i,0} \phi_i(x),$$

where the inner product $\langle f(x), g(x) \rangle = \int f(x) g(x) dx$. Therefore,

$$H(x) = \frac{\sum_i \left(\sum_j c_{i,j} \langle y, \phi_j(y) \rangle \right) \phi_i(x)}{\langle 1, \phi_0(y) \rangle \sum_i c_{i,0} \phi_i(x)}.$$

When the Legendre polynomial basis is used and $y \in [-1, 1]$, the formula can be further simplified to

$$H(x) = \frac{\sum_i (c_{i,1} \langle y, \phi_1(y) \rangle) \phi_i(x)}{\langle 1, \phi_0(y) \rangle \sum_i c_{i,0} \phi_i(x)}$$

as y is one of the (scaled) basis functions.

For two-dimensional implementations, the data set $\{(x_n, y_n)\}_{n=1}^N$ can be efficiently transformed into a copula data set. The transformed data set satisfies the condition that the marginal distribution of X follows the uniform distribution $U[0, 1]$ and $\sum_i c_{i,0} \phi_i(x) = 1$. Numerically, the copula transformation is preferred for better numerical stability (and accuracy) properties, as when using the estimated coefficients $\hat{c}_{i,j}$, the function $\sum_i \hat{c}_{i,0} \phi_i(x)$ may not always be positive, and small perturbations of this function may cause large errors in the resulting $H(x)$ estimate. We present a stable bump-hunting formulation when using the Legendre polynomial basis for a copula physical domain data set.

Algorithm 3 (Bump Hunting): Assume the data set $\{(x_n, y_n)\}_{n=1}^N$ is a copula data set in $[0, 1]^2$. One can construct the random coefficient matrix C using the (normalized) Legendre polynomial basis (efficiently using fast Legendre transforms) and the bump function $H(x)$ is given by

$$H(x) = \frac{\sum_i (c_{i,1} \langle y, \phi_1(y) \rangle) \phi_i(x)}{\langle 1, \phi_0(y) \rangle},$$

For more general basis choices with $\phi_0(x) = \frac{1}{\|1\|}$, the bump function is given by

$$H(x) = \frac{\sum_i \left(\sum_j c_{i,j} \langle y, \phi_j(y) \rangle \right) \phi_i(x)}{\langle 1, \phi_0(y) \rangle}.$$

The formulas for $G(y)$ can be derived similarly and we skip the details.

3.2.2. Low Dimensional Structures $H(x) = G(y)$. When the physical domain data (x, y) are generated using the equation $y = \sin(x) + \epsilon$ where $\epsilon \sim N(0, \delta)$, bump hunting can effectively reveal the deterministic relationship $y = \sin(x)$. However, when the data pairs are generated around a circle $x^2 + y^2 = 1$ with some independent random perturbations to X and Y , respectively, because of the nonlinearity in the low-dimensional geometric structure (circle), the bump functions $\mathbb{E}[Y|X = x]$ and $\mathbb{E}[X|Y = y]$ are approximately given by the perpendicular lines $x = 0$ and $y = 0$, respectively. Neither of these corresponds to the low-dimensional structure we are searching for.

Finding general low-dimensional structures hidden in the multi-variable probability density function is an open problem and requires assumptions on many factors, including the underlying geometric structure and properties of the random noise. For the one-dimensional structure $H(x) = G(y)$ in a two-dimensional data set, an intuitive idea is to search for the functions $H(x)$ and $G(y)$ such that

$$\mathbb{E}[G(Y) - H(X)|X = x] = 0 \quad \text{and} \quad \mathbb{E}[G(Y) - H(X)|Y = y] = 0.$$

Or more generally, $\mathbb{E}[H(X) - G(Y)|(\cos(\theta)X + \sin(\theta)Y = \cos(\theta)x + \sin(\theta)y)] = 0$ for all possible angles θ . This is possible when data are exactly located on the low-dimensional manifold and there is no noise. However, for noisy data, there are existence, uniqueness, regularity issues, as well as computational efficiency and stability issues with this formulation. For example, consider $x = 1 + \epsilon$ where $\epsilon \sim N(0, \delta)$ and the deterministic relation is given by $x = 1$. If one studies x^2 , a simple calculation shows $\mathbb{E}(x^2 - 1) \neq 0$ and one gets a (slightly) different

relation. Another example is $y = \sin(x) + \epsilon$, where $-1 \leq x \leq 1$ and $\epsilon \sim N(0, \delta)$. The deterministic relation using $\mathbb{E}[Y|X = x]$ gives the function $y = \sin(x)$, while bump hunting returns a (slightly) different relation if we use $\mathbb{E}(X|Y = y)$.

In this paper, we introduce a specific definition of the low-dimensional structure given by the relation $H(x) = G(y)$, which is well-defined and efficient to calculate. We first present the algorithms (based on existing statistical data analysis tools).

Algorithm 4.1 (CCA - Low Dimensional Structure): For a given data set $\{(x_n, y_n)\}_{n=1}^N$, (not necessarily a copula data set in $[0, 1]^2$), construct the frequency domain data sets

$$X = \{\phi_0(x_i), \phi_1(x_i), \dots, \phi_K(x_i)\} \quad \text{and} \quad Y = \{\phi_0(y_i), \phi_1(y_i), \dots, \phi_K(y_i)\}, \quad i = 1, \dots, N.$$

Apply existing canonical correlation analysis (CCA) tools, for example, the Matlab function

$$[\vec{A}, \vec{B}, \vec{r}, \vec{U}, \vec{V}] = \text{canoncorr}(X, Y).$$

Then the CCA-low-dimensional structure (CCA-LDS) is given by $H(x) = G(y)$ where

$$H(x) = \sum_{k=0}^K A(k, 1) \phi_k(x), \quad G(y) = \lambda \sum_{k=0}^K B(k, 1) \phi_k(y),$$

and λ is a constant which can be computed using a simple linear fit.

Note that most existing CCA tools do not consider the special structures of the basis functions. As the CCA algorithm is based on the singular value decomposition algorithm, to take advantage of existing fast transformation algorithms (e.g., NUFFT or fast Haar transform), we present a slightly modified algorithm for finding $A(:, 1)$ and $B(:, 1)$.

Algorithm 4.2 (SVD - Low Dimensional Structure): For a given data set $\{(x_n, y_n)\}_{n=1}^N$, (not necessarily a copula data set in $[0, 1]^2$), construct the frequency domain coefficient and variance matrices \hat{C} , $\tilde{\Sigma}_{XX}$, $\tilde{\Sigma}_{YY}$, and $\tilde{\Sigma}_{XY}$ using a fast transformation algorithm. Apply existing singular value decomposition (SVD) tools to the covariance matrix $\tilde{\Sigma}_{XY}$, and denote the left and right singular vectors corresponding to the largest singular value as \vec{c} and \vec{d} . Define $\vec{\omega} = \tilde{\Sigma}_{XX}^{-1/2} \vec{c}$ and $\vec{\beta} = \tilde{\Sigma}_{YY}^{-1/2} \vec{d}$. Then the SVD-low-dimensional structure (SVD-LDS) is given by $H(x) = G(y)$ where

$$(3.3) \quad H(x) = \sum_{k=1}^K \omega_k \phi_k(x), \quad G(y) = \lambda \sum_{k=1}^K \beta_k \phi_k(y) + \gamma,$$

and λ and γ are constants that can be computed using a simple linear fit.

Comment: Note that the index k starts from 0 in Algorithm 4.1, but from 1 in Algorithm 4.2. Also, Algorithm 4.2 can be more efficient due to the application of fast transformation algorithms. In Algorithms 4.1 and 4.2, the coefficients $A(k, 1)$, $B(k, 1)$, ω_k , and β_k are uniquely determined. However, the coefficients λ and γ depend on how the linear fit problem is formulated. In the current implementation, we solve the least squares optimization problem

$$\sum_{n=1}^N \left(\sum_{k=1}^K \omega_k \phi_k(x_n) - (\lambda \sum_{k=1}^K \beta_k \phi_k(y_n) + \gamma) \right)^2.$$

An alternative least squares problem is

$$\sum_{n=1}^N \left(\tilde{\lambda} \sum_{k=1}^K \omega_k \phi_k(x_n) + \tilde{\gamma} - \sum_{k=1}^K \beta_k \phi_k(y_n) \right)^2$$

and the functions $H(x)$ and $G(y)$ are then defined as

$$H(x) = \tilde{\lambda} \sum_{k=1}^K \omega_k \phi_k(x_n) + \tilde{\gamma} \quad \text{and} \quad G(y) = \sum_{k=1}^K \beta_k \phi_k(y).$$

As we will demonstrate in [section 4](#), the two different formulations define different low-dimensional manifold structures. Indeed, the proper definition of physically relevant low-dimensional structures in the data requires knowledge of the structures and assumptions of the data set and noise.

3.2.3. Algebraic Interpretation. We explain the algebraic/geometric meaning of the relation equation $H(x) = G(y)$ and its connections to the bump hunting type conditions

$$(3.4) \quad \mathbb{E}[H(X) - G(Y)|X = x] = 0 \quad \text{and} \quad \mathbb{E}[H(X) - G(Y)|Y = y] = 0.$$

As there are no $\{H(x), G(y)\}$ that exactly satisfy both conditions in Eq. (3.4), in the remainder of this section, we show that the relation $H(x) = G(y)$ from Algorithm 4.2 (the same as that from Algorithm 4.1) represents a particular “best” least squares type solution to the inconsistent system in Eq. (3.4).

We first consider a fixed x and the condition $\mathbb{E}[G(Y) - H(X)|X = x] = 0$. We start with

$$\int (G(y) - H(x)) \left(\sum_{i,j} c_{i,j} \phi_i(x) \phi_j(y) \right) dy = 0,$$

or equivalently,

$$\int G(y) \left(\sum_{i,j} c_{i,j} \phi_i(x) \phi_j(y) \right) dy = \int H(x) \left(\sum_{i,j} c_{i,j} \phi_i(x) \phi_j(y) \right) dy = H(x) P_X(x),$$

where $P_X(x)$ is the marginal probability density function of the random variable X . When $X \sim U[0, 1]$, $P_X(x) = 1$. Next, using the expansions

$$H(x) = \sum_{k=0}^K \omega_k \phi_k(x) \quad \text{and} \quad G(y) = \sum_{k=0}^K \beta_k \phi_k(y)$$

and the orthogonality of the basis functions, we have the equations for the coefficients

$$C \begin{bmatrix} \beta_0 \\ \beta_1 \\ \vdots \\ \beta_K \end{bmatrix} = \left(\Sigma_{XX} + \begin{bmatrix} c_{0,0} \\ c_{1,0} \\ \vdots \\ c_{K,0} \end{bmatrix} [c_{0,0}, c_{1,0}, \dots, c_{K,0}] \right) \begin{bmatrix} \omega_0 \\ \omega_1 \\ \vdots \\ \omega_K \end{bmatrix},$$

where C is the frequency domain coefficient matrix and Σ_{XX} is the variance matrix defined in subsection 2.3. As $\phi_0(x)$ is the constant function, we further simplify the relation equation by introducing \tilde{C}

$$C = \begin{bmatrix} c_{0,0} & c_{0,1} & \cdots & c_{0,K} \\ c_{1,0} & & & \\ \vdots & & \tilde{C} & \\ c_{K,0} & & & \end{bmatrix}$$

and consider the new relation equation

$$\left[\beta_0 \begin{bmatrix} \sum_{k=0}^K c_{0,k} \beta_k \\ c_{1,0} \\ \vdots \\ c_{K,0} \end{bmatrix} + \tilde{C} \begin{bmatrix} \beta_1 \\ \vdots \\ \beta_K \end{bmatrix} \right] = \left[\tilde{\Sigma}_{XX} \begin{bmatrix} \omega_1 \\ \vdots \\ \omega_K \end{bmatrix} + (\sum_{k=0}^K c_{k,0} \omega_k) \begin{bmatrix} c_{1,0} \\ \vdots \\ c_{K,0} \end{bmatrix} \right].$$

Using the first equation $\sum_{k=0}^K c_{0,k} \beta_k = \sum_{k=0}^K c_{k,0} \omega_k$, we can translate the second vector equation system into

$$(\beta_0 - \sum_{k=0}^K c_{0,k} \beta_k) \begin{bmatrix} c_{1,0} \\ \vdots \\ c_{K,0} \end{bmatrix} + \tilde{C} \begin{bmatrix} \beta_1 \\ \vdots \\ \beta_K \end{bmatrix} = \tilde{\Sigma}_{XX} \begin{bmatrix} \omega_1 \\ \vdots \\ \omega_K \end{bmatrix}.$$

Further simplifying the equation using the assumption that $\phi_0(x)$ is a constant function, we have

$$(\tilde{C} - \begin{bmatrix} c_{1,0} \\ \vdots \\ c_{K,0} \end{bmatrix} [c_{0,1}, \dots, c_{0,K}]) \begin{bmatrix} \beta_1 \\ \vdots \\ \beta_K \end{bmatrix} = \tilde{\Sigma}_{XX} \begin{bmatrix} \omega_1 \\ \vdots \\ \omega_K \end{bmatrix},$$

or equivalently,

$$(3.5) \quad \tilde{\Sigma}_{XY} \begin{bmatrix} \beta_1 \\ \vdots \\ \beta_K \end{bmatrix} = \tilde{\Sigma}_{XX} \begin{bmatrix} \omega_1 \\ \vdots \\ \omega_K \end{bmatrix}.$$

Similarly, if we fix y and consider the equation $\mathbb{E}[\tilde{G}(Y) - \tilde{H}(X)|Y = y] = 0$, we get the linear system

$$(3.6) \quad \tilde{\Sigma}_{XY}^T \begin{bmatrix} \tilde{\omega}_1 \\ \vdots \\ \tilde{\omega}_K \end{bmatrix} = \tilde{\Sigma}_{YY} \begin{bmatrix} \tilde{\beta}_1 \\ \vdots \\ \tilde{\beta}_K \end{bmatrix}.$$

We used the notation \tilde{H} , \tilde{G} , $\tilde{\omega}$ and $\tilde{\beta}$ to represent a new set of functions and vectors. If we require the new set to be the same as the original ones, we will have

$$\left(\tilde{\Sigma}_{YY}^{-1} \tilde{\Sigma}_{XY}^T \tilde{\Sigma}_{XX}^{-1} \tilde{\Sigma}_{XY} \right) \begin{bmatrix} \tilde{\beta}_1 \\ \vdots \\ \tilde{\beta}_K \end{bmatrix} = \begin{bmatrix} \tilde{\beta}_1 \\ \vdots \\ \tilde{\beta}_K \end{bmatrix}$$

and

$$\left(\tilde{\Sigma}_{XX}^{-1}\tilde{\Sigma}_{XY}\tilde{\Sigma}_{YY}^{-1}\tilde{\Sigma}_{XY}^T\right)\begin{bmatrix}\tilde{\omega}_1 \\ \vdots \\ \tilde{\omega}_K\end{bmatrix}=\begin{bmatrix}\tilde{\omega}_1 \\ \vdots \\ \tilde{\omega}_K\end{bmatrix},$$

i.e., 1 is an eigenvalue of the matrix $\tilde{\Sigma}_{XX}^{-1}\tilde{\Sigma}_{XY}\tilde{\Sigma}_{YY}^{-1}\tilde{\Sigma}_{XY}^T$. Such solutions unfortunately may not exist. Instead of finding $\tilde{H} = H$, $\tilde{G} = G$, $\tilde{\omega} = \omega$, and $\tilde{\beta} = \beta$, SVD-LDS and CCA-LDS solve an optimization problem. In the frequency domain, consider a given set of coefficients $[\beta_1, \beta_2, \dots, \beta_K]$ (a given function $G(y)$). Define

$$\vec{c} = \Sigma_{YY}^{\frac{1}{2}} \begin{bmatrix} \beta_1 \\ \vdots \\ \beta_K \end{bmatrix}$$

and assume $\|\vec{c}\| = 1$ (normalized $G(y)$ using a particular norm). One can compute the

coefficient vector $\vec{d} = \Sigma_{XX}^{\frac{1}{2}} \begin{bmatrix} \omega_1 \\ \vdots \\ \omega_K \end{bmatrix}$ (a resulting $H(x)$ function) using Eq. (3.5) to get

$$\vec{d} = \Sigma_{XX}^{-1/2} \Sigma_{XY} \Sigma_{YY}^{-\frac{1}{2}} \vec{c}.$$

Then using \vec{d} and Eq. (3.6), one can get a new coefficient vector

$$\tilde{c} = \Sigma_{YY}^{-\frac{1}{2}} \Sigma_{YX} \Sigma_{XX}^{-\frac{1}{2}} \vec{d}$$

(a new function \tilde{H}). We have the following theorem

Theorem 3.5. *The algorithms 4.1 and 4.2 return a vector $\|\vec{c}\| = 1$ which minimizes*

$$\|\tilde{c} - \vec{c}\| = \|(\Sigma_{YY}^{-\frac{1}{2}} \Sigma_{YX} \Sigma_{XX}^{-1} \Sigma_{XY} \Sigma_{YY}^{-\frac{1}{2}} - I) \vec{c}\|.$$

A similar result can be derived when one starts from \vec{d} and minimizes $\|\tilde{d} - \vec{d}\|$. Comparing the results with standard CCA analysis, we summarize our results in the following theorem for the vectors $\vec{\beta}$, $\vec{\omega}$, \vec{c} , and \vec{d} .

Theorem 3.6. *The solution vectors $\vec{\beta}$, $\vec{\omega}$, \vec{c} , and \vec{d} from Algorithms 4.1 and 4.2 have the following properties.*

1. *The vectors $\vec{\beta}$ and $\vec{\omega}$ maximize*

$$\rho(\vec{\beta}, \vec{\omega}) = \frac{\vec{\beta}^T \tilde{\Sigma}_{XY} \vec{\omega}}{\sqrt{\vec{\beta}^T \tilde{\Sigma}_{XX} \vec{\beta}} \sqrt{\vec{\omega}^T \tilde{\Sigma}_{YY} \vec{\omega}}},$$

or in statistical language,

$$\operatorname{argmax}_{\vec{\beta}, \vec{\omega}} \operatorname{Corr}(\vec{\beta}^T \phi(x), \vec{\omega}^T \phi(y)) = \operatorname{argmax}_{\vec{\beta}, \vec{\omega}} \frac{E[(\vec{\beta}^T \phi(x))(\vec{\omega}^T \phi(y))]}{\sqrt{E[(\vec{\beta}^T \phi(x))^2] E[(\vec{\omega}^T \phi(y))^2]}}.$$

2. The vectors \vec{c} and \vec{d} maximize

$$\rho = \frac{\vec{c}^T \Sigma_{XX}^{-\frac{1}{2}} \tilde{\Sigma}_{XY} \Sigma_{YY}^{-\frac{1}{2}} \vec{d}}{\sqrt{\vec{c}^T \vec{c}} \sqrt{\vec{d}^T \vec{d}}},$$

where $\vec{c} = \Sigma_{YY}^{-\frac{1}{2}} \vec{\beta}$ and $\vec{d} = \Sigma_{XX}^{-\frac{1}{2}} \vec{\omega}$.

3. \vec{c} and \vec{d} are the singular vectors of the correlation matrix Σ_{XY} .

4. \vec{c} and $\Sigma_{XX}^{-\frac{1}{2}} \tilde{\Sigma}_{XY} \Sigma_{YY}^{-\frac{1}{2}} \vec{d}$ are collinear, \vec{d} and $\Sigma_{YY}^{-\frac{1}{2}} \tilde{\Sigma}_{YX} \Sigma_{XX}^{-\frac{1}{2}} \vec{c}$ are collinear.

As we will demonstrate in [section 4](#), Algorithms 4.1 and 4.2 can be applied to find specific low-dimensional structures described by $H(x) = G(y)$, especially when both $H(x)$ and $G(y)$ only contain low-frequency modes. However, we found that the current formulations are not the most stable numerically. A more serious problem is that although the new nonlinear relation $H(x) = G(y)$ is more general compared with the relations $y = f(x)$ and $x = g(y)$ in the bump hunting algorithms, some relations cannot be described by $H(x) = G(y)$. For example, none of the proposed algorithms can effectively find the (polynomial type) relation equation $x \cdot y = 0$ or more general algebraic varieties. For more general low-dimensional structures described by the equation $H(x, y) = 0$, the theoretical analysis and efficient and stable numerical solutions of a well-defined optimization problem are currently being studied, and results will be presented in the future.

4. Preliminary Numerical Results. In this section, we present some preliminary numerical results for the frequency domain-based statistical data analysis algorithms.

4.1. Dependency Test. We demonstrate the statistical power of the frequency domain dependency test algorithms Max-FiT and SVD-FiT. We present the results for the Fourier series, Legendre polynomials and Haar wavelet basis functions, and compare them with those from the Walsh functions-based BET algorithms in [\[63\]](#) for 6 types of manufactured dependent data sets in [Table 4.1](#), where $U \sim \text{Uniform}[0, 1]$, $W \sim \text{MultiBern}(\{1, 2, 3\}, (1/3, 1/3, 1/3))$, $V_1 \sim \text{Bern}(\{2, 4\}, (1/2, 1/2))$, $V_2 \sim \text{MultiBern}(\{1, 3, 5\}, (1/3, 1/3, 1/3))$, $G_1, G_2 \sim N(0, 1/4)$, and $\epsilon, \epsilon',$ and $\epsilon'' \sim N(0, \sigma^2)$. Sampled data sets for different σ choices are plotted in [Figure 4.1](#).

Table 4.1: Manufactured dependent data sets for independence tests.

Linear	$X = U$	$Y = 2X + 10\epsilon$
Parabolic	$X = U$	$Y = (X - 0.5)^2 + 1.5\epsilon$
Circular	$X = 5 \cos \theta + 40\epsilon$	$Y = 5 \sin \theta + 40\epsilon'$
Sine	$X = U$	$Y = \sin(2\pi X) + 15\epsilon$
Checkerboard	$X = W + \epsilon$	$Y = \begin{cases} V_1 + \epsilon' & \text{if } W = 2 \\ V_2 + \epsilon'' & \text{otherwise.} \end{cases}$
Local	$X = G_1$	$Y = \begin{cases} X + \epsilon' & \text{if } 0 \leq G_1, G_2 \leq 1 \\ G_2 & \text{otherwise.} \end{cases}$

In [Figure 4.2](#), we show the statistical power of the Max-FiT and SVD-FiT algorithms using different basis functions. The statistical power is the probability that the test correctly

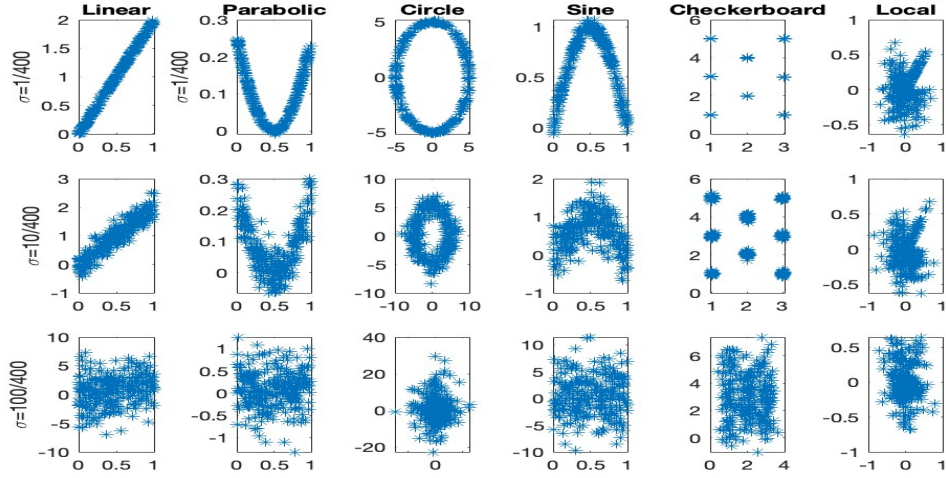


Figure 4.1: Six dependent random data sets for different σ values $1/400$ (row 1), $10/400$ (row 2), and $100/400$ (row 3).

rejects the independence hypothesis for a dependent data set. In the plot, the x -axis shows the noise level $\sigma = x/40$ and the y -axis shows the statistical power. For each noise level, we generate 1000 random data sets to estimate the probability. Each data set has 256 data points $\{(x_n, y_n)\}_{n=1}^{256}$. We simulate the null distributions of the independent cases for different basis choices and statistics using a permutation test [3, 13, 20, 21] with 200 permutations for each case. Note that the computationally expensive permutation tests can be avoided in future implementations by analytically approximating the null distributions using asymptotic analysis. For the manufactured examples, we found that the Legendre polynomial-based algorithms (“Legendre Max” and “Legendre SVD”) in general outperform methods using other bases. Methods based on the local Haar basis functions often perform poorly (“Haar Max” and “Nonstandard Haar”), and the statistical power of the global “Haar SVD” method is identical to that of the “Walsh SVD” algorithm, which suggests that an optimal independence test statistic needs to consider the global properties of the manufactured data sets.

In Figure 4.3, we present the statistical power of the algorithms for independent data sets. The experiments were repeated 10 times (x -axis) and each experiment considered 1000 random data sets each containing 256 data points $\{(x_n, y_n)\}_{n=1}^{256}$. The results assess the type I error of rejecting the independence hypothesis when it is actually true. As we set the p -value threshold at 5%, the statistical power of each algorithm (y -axis) correctly oscillates around 5%.

In addition to manufactured data sets, we also applied the algorithms to real world data sets. In Table 4.2, we study the (dependent) galactic coordinates of the 256 brightest stars in the night sky from [63]. The galactic coordinates are essentially spherical coordinates with the Sun at the center. We present the p -values for different algorithms. If the p -value is less than 5%, one can confidently claim that the coordinates are not independent (rejecting the

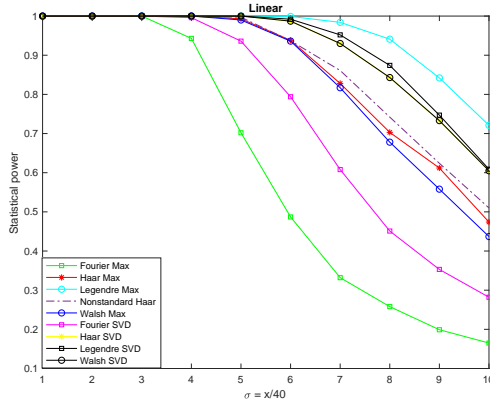
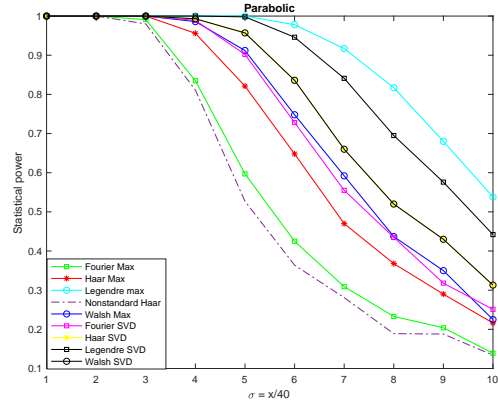
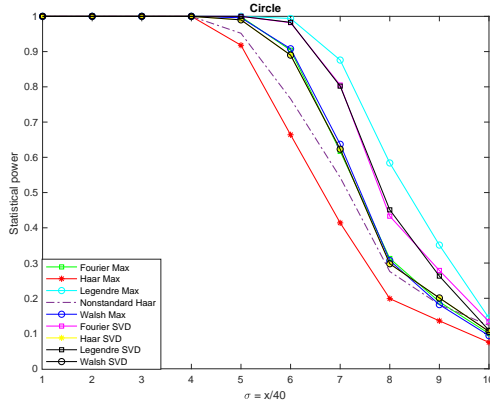
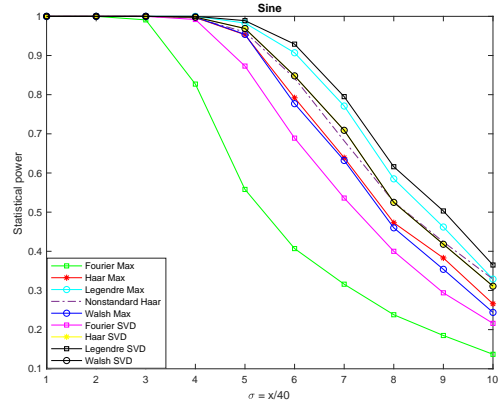
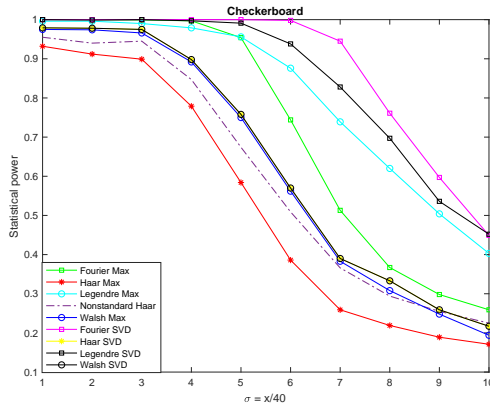
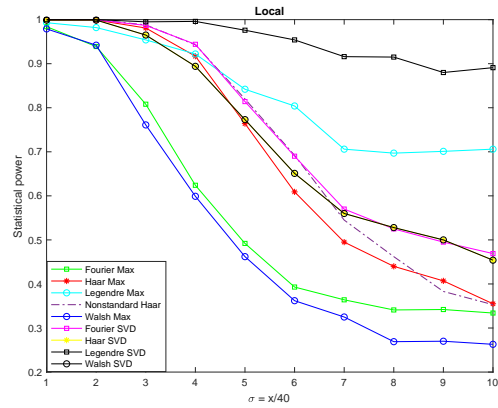
(a) *Linear*(b) *Parabolic*(c) *Circle*(d) *Sine*(e) *Checkerboard*(f) *Local*

Figure 4.2: Statistical power of Max-FiT and SVD-FiT for different bases.

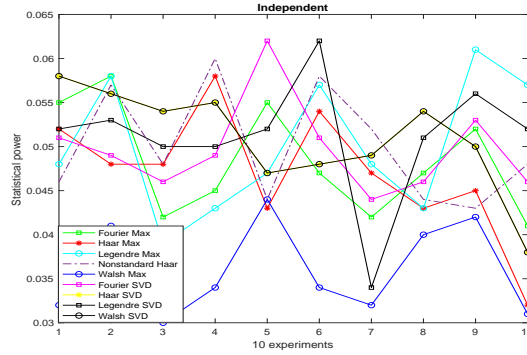


Figure 4.3: Statistical power of Max-FiT and SVD-FiT for independent data sets.

Table 4.2: p-values from different algorithms for galactic coordinates of 256 brightest stars.

	p-value		p-value
Fourier Max	0.03	Fourier SVD	0.000
Haar Max	0.025	Haar SVD	0.005
Legendre Max	0.040	Legendre SVD	0.000
Nonstandard Haar	0.1400		
Walsh Max	0.005	Walsh SVD	0.005

independence hypothesis). Clearly, some basis choices can better identify whether the data are independent or not. The Max-FiT algorithm using the nonstandard Haar wavelet basis (“Nonstandard Haar”) is not competitive due to the local properties of the nonstandard Haar basis functions. Also, as the nonstandard Haar basis is not constructed using the tensor product of one-dimensional basis functions, one cannot apply the SVD-FiT algorithm to “Nonstandard Haar” to get global information and improve the performance. However, the “sparse grid” nonstandard Haar wavelet basis may allow the study of high-dimensional data sets located on a low-dimensional manifold. Therefore, an ongoing research topic is how to define a global statistic based on the adaptive nonstandard Haar wavelet basis for higher-dimensional data sets. Results along this direction will be reported in future publications.

In our final example for the independence test, we study whether there exists a connection between the daily percentage alteration in temperature in New York City and that in the Dow Jones Industrial Average (DJI) in 2019. For Day i , we define $x_i = (\text{highest temperature} - \text{lowest temperature}) / (\text{lowest temperature})$ and $y_i = (\text{highest DJI} - \text{lowest DJI}) / (\text{lowest DJI})$. In Table 4.3, we show the p -values from different algorithms. We observe significant differences in the results when different basis choices are used. The “smooth” and “global” basis choices (Fourier series and Legendre polynomials) suggest that the data are independent, while methods using the Haar and Walsh wavelet bases seem to suggest that the data are related. One conjecture is that there exists a “local” relation in the variables which states that when there is an extremely large percentage change in the temperature, the change in the DJI tends to

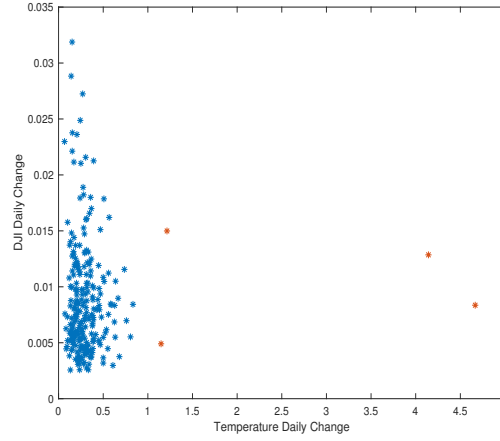


Figure 4.4: Temperature alternation vs DJI alternation.

Table 4.3: p-values for testing dependency of changes in temperature and in DJI index.

	p-value		p-value
Fourier Max	0.275	Fourier SVD	0.510
Haar Max	0.060	Haar SVD	0.015
Legendre Max	0.315	Legendre SVD	0.635
Nonstandard Haar	0.005		
Walsh Max	0.060	Walsh SVD	0.015

be milder. This local relation can be captured by the Walsh and Haar basis functions, but is smoothed out by the more global and smooth Legendre and Fourier bases. To validate this conjecture, we remove the 4 data points with the most significant temperature variations with $x_i > 1$ (red points in Figure 4.4), and re-calculate the p-values for the new data set. The results are shown in Table 4.4. All algorithms suggest that the new data sets are now more likely to be independent. This example demonstrates the challenges of accurate independence

Table 4.4: p-values for testing dependency of changes in temperature and in DJI index after removing 4 points.

	p-value		p-value
Fourier Max	0.310	Fourier SVD	0.520
Haar Max	0.205	Haar SVD	0.110
Legendre Max	0.215	Legendre SVD	0.500
Nonstandard Haar	0.100		
Walsh Max	0.285	Walsh SVD	0.110

testing when the noise level is high (see also the differences in statistical power for large values σ in Figure 4.2) or the relationships are complicated.

4.2. Finding Low-Dimensional Structures. We first apply the bump hunting algorithm (Algorithm 3) to 5 manufactured examples shown in Figure 4.5. The (dependent) random

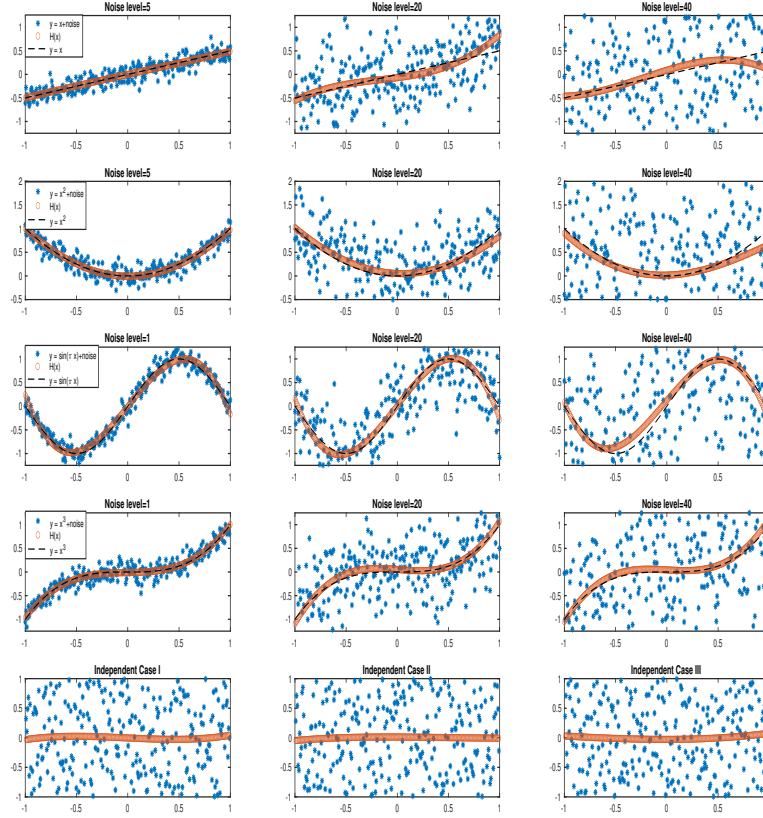


Figure 4.5: Bump Hunting results for different noise levels.

data sets (blue asterisks) are generated using $y = x + \epsilon_1$ (linear), $y = x^2 + \epsilon_2$ (parabolic), $y = \sin(x) + \epsilon_3$ (sine) and $y = x^3 + \epsilon_4$ (cubic), respectively, where $\epsilon_i \sim l * N(0, 1)$, $i = 1, 2, 3, 4$. For each example, we consider three different noise levels given by $l = 5$, $l = 20$, and $l = 40$. For comparison reasons, we also consider 3 independent data sets sampled from the distribution $U([-1, 1]^2)$ shown in the last row of Figure 4.5. Each data set contains a total number of 256 data points. In the bump hunting algorithm implementation, we use the Legendre polynomials so that the identified low-dimensional structure is described by a polynomial function. For all cases, the frequency domain-based bump hunting algorithm (Algorithm 3) performs well for finding the well-defined bump functions, and the computed bump function (red circles)

remains close to the ground truth (black dashed lines) even at high noise levels.

Next, we study the algebraic relations in the form of $H(x) = G(y)$ derived by solving the specific optimization formulation discussed in Section 3.2. As polynomial approximations and the zeros of polynomial systems (algebraic varieties) are well-studied by the mathematics community, we therefore consider the manufactured data sets generated using polynomial relations listed in Table 4.5, with random noises $\epsilon_i \sim N(0, l/40)$, $i = 1, \dots, 6$ and 3 different noise levels $l = 1$, $l = 10$, and $l = 20$, respectively. Each data set contains 256 data points (red asterisks in Fig. 4.6). We have applied both Algorithm 4.1 (CCA-LDS) and Algorithm

Table 4.5: Finding low-dimensional structures in the form of $H(x) = G(y)$.

$H(x) = G(y)$	x	y	θ
$x^2 + y^2 = 4$	$x = 2 \sin \theta + \epsilon_1$	$y = 2 \cos \theta + \epsilon_2$	$[0, 2\pi]$
$y^2 = 4x^2(1 - x^2)$	$x = \sin \theta$	$y = \sin(2\theta) + \epsilon_3$	$[0, 2\pi]$
$x^2 - y^2 = 1$	$x = \frac{\cos \theta}{\sqrt{\cos(2\theta)}}$	$y = \frac{\sin \theta}{\sqrt{\cos(2\theta)}} + \epsilon_4$	$[-0.69, 0.68] \cup [2.46, 3.83]$
$x^2 = y^2$	$x \sim U(-1, 1)$	$y = \pm x + \epsilon_{5,6}$	

4.2 (SVD-LDS) to the cases listed in Table 4.5. As the results from Algorithm 4.1 and Algorithm 4.2 are very similar, we only plot the identified curves (blue curve) from Algorithm 4.1 in Fig. 4.6. For low noise levels, the algorithms accurately capture the underlying low-dimensional manifolds. However, as the noise level increases, the accuracy of the identified low-dimensional curves deteriorates.

Note that for the last three cases in Table 4.5, we only added noise to the y -variable. In the next experiment, we show how the results change when the noise is added only to the x -variable as demonstrated in Table 4.6. We use the same random noise ϵ_i settings as those in

Table 4.6: Adding noise only to the x -variable

$H(x) = G(y)$	x	y	θ
$y^2 = 4x^2(1 - x^2)$	$x = \sin \theta + \epsilon_1$	$y = \sin(2\theta)$	$[0, 2\pi]$
$x^2 - y^2 = 1$	$x = \frac{\cos \theta}{\sqrt{\cos(2\theta)}} + \epsilon_2$	$y = \frac{\sin \theta}{\sqrt{\cos(2\theta)}}$	$[-0.69, 0.68] \cup [2.46, 3.83]$
$x^2 = y^2$	$x = \pm y + \epsilon_{3,4}$	$y \sim U(-1, 1)$	

Table 4.5. The generated data sets (red asterisks) and identified low-dimensional structures (blue curves) are presented in Figure 4.7. For low noise settings, Algorithms 4.1 and 4.2 can still correctly capture the ground truth. However, for high noise levels, as the relation $y^2 = 4x^2(1 - x^2)$ is more nonlinear in x than in y , the identified curves do not correctly capture the underlying curve used to generate the data sets.

We also find that the current Algorithms 4.1 and 4.2 are sensitive to random noises for cases with high noise levels. In Figure 4.8, we consider the relation $y^2 = 4x^2(1 - x^2)$ with noise only added to the x -variable as presented in Table 4.6. For the noise level $l = 10$, we generate three data sets using different seeds for the random number generator. One can

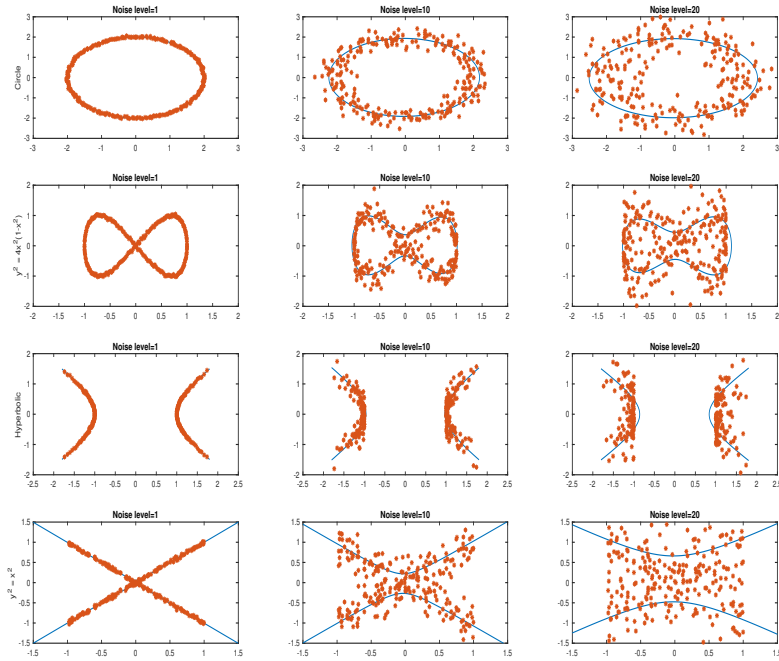
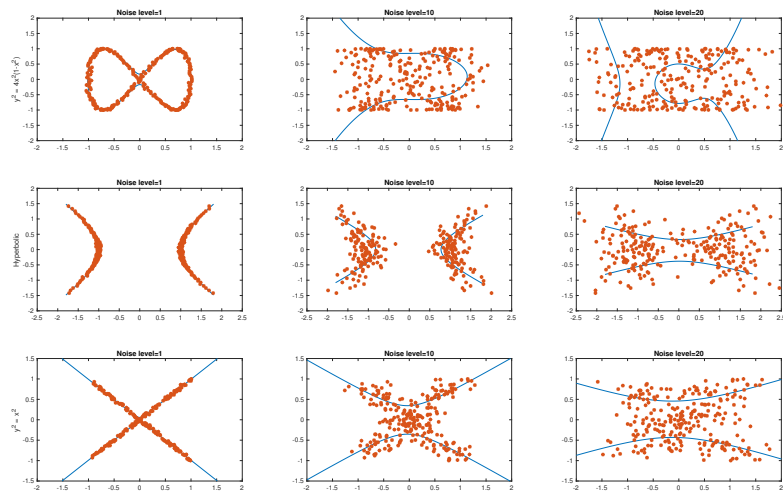


Figure 4.6: CCA-LDS results for data sets with different noise levels.

Figure 4.7: CCA-LDS results for data sets with noise only added to x .

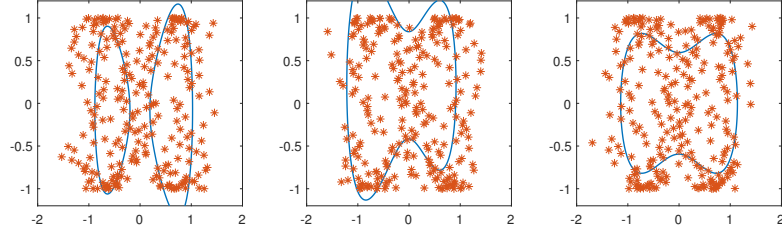


Figure 4.8: CCA-LDS results for relation $y^2 = 4x^2(1 - x^2)$ with noise only added to the x -variable, noise level $l = 10$. Three data sets are obtained using different seeds for the random number generator.

observe the differences in the identified low-dimensional manifolds (blue curves) although the same relation and noise level are used to generate the random data sets. This also reveals the challenges in numerically identifying the underlying nonlinear low-dimensional structures in high noise settings.

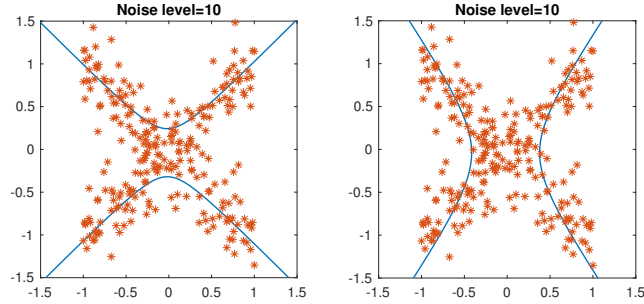


Figure 4.9: Identified low-dimensional structures using different linear fit strategies.

Finally, we show the impact of different linear fit strategies, $G(y) = \lambda H(x) + \gamma$ and

$\tilde{\lambda}G(y) + \tilde{\gamma} = H(x)$, on the identified low-dimensional manifold in Figure 4.9. We consider the symmetric relation $x^2 = y^2$ where the noise is added to the y -variable only. The noise level is set to $l = 10$. The data set contains 256 points. In the left panel, we show the identified curve when the standard linear fit $G(y) = \lambda H(x) + \gamma$ is applied. In the right panel, we show the result when the alternative linear fit $\tilde{\lambda}G(y) + \tilde{\gamma} = H(x)$ is used.

Our preliminary research on the algebraic relations in the form of $H(x) = G(y)$ has revealed the challenges in finding low-dimensional structures in high-dimensional data sets. The current optimization formulation has some nice existence, uniqueness, and regularity properties, and it can be solved efficiently using existing L_2 norm-based singular value decomposition or canonical-correlation analysis tools. However, the current formulation has stability issues and the identified low-dimensional algebraic structure appears to be sensitive to noise structures (e.g., how the noise is added and noise levels). Some of these issues are being studied for more general algebraic relations $H(x, y) = 0$ and results will be reported in the future.

5. Summary and Future Work. In this paper, by introducing different orthonormal basis functions and applying fast transformation algorithms, we construct the frequency domain expansion coefficients and higher-order moments of the probability density function of physical domain data. We show how the new set of frequency domain data can be utilized to address some fundamental questions arising in data analysis, including testing the dependence between variables in the data set and identifying any low-dimensional algebraic relations in dependent data. Numerical experiments are presented to demonstrate the performance of the resulting numerical algorithms.

Revisiting the fundamental data analysis questions from the frequency/spectral domains and applied analysis perspectives has provided us with powerful tools to address some interesting and challenging questions. One of our current projects is to generalize the frequency domain statistical analysis techniques to high-dimensional data sets, by properly choosing an appropriate set of adaptive basis functions for high-dimensional data with low-rank or low-dimensional compressible features. Another project is to design improved statistics that better distinguish the null distribution from the alternative distribution. Results along these directions will be reported in the future.

Acknowledgments. We thankfully acknowledge the support from the National Science Foundation under Grants #2152289 (HB, JH, JS, KZ, WZ), #2012451 (SC, JH, JS), and #2152070 (YW). Any opinions, findings, and conclusions or recommendations expressed in this paper are those of the authors and do not necessarily reflect the views of the National Science Foundation.

REFERENCES

- [1] M. ABRAMOWITZ, I. A. STEGUN, AND R. H. ROMER, *Handbook of mathematical functions with formulas, graphs, and mathematical tables*, 1988.
- [2] G. W. ANDERSON, A. GUIONNET, AND O. ZEITOUNI, *An introduction to random matrices*, no. 118, Cambridge university press, 2010.
- [3] D. H. ANNIS, *Permutation, parametric, and bootstrap tests of hypotheses*, 2005.
- [4] Z. BAI AND J. W. SILVERSTEIN, *Spectral analysis of large dimensional random matrices*, vol. 20, Springer, 2010.

- [5] S. BALAKRISHNAN AND L. WASSERMAN, *Hypothesis testing for densities and high-dimensional multinomials: Sharp local minimax rates*, The Annals of Statistics, 47 (2019), pp. 1893 – 1927, <https://doi.org/10.1214/18-AOS1729>.
- [6] K. G. BEAUCHAMP AND C. YUEN, *Walsh functions and their applications*, IEEE Transactions on Systems, Man, and Cybernetics, (1976), pp. 794–795.
- [7] T. B. BERRETT, I. KONTOYIANNIS, AND R. J. SAMWORTH, *Optimal rates for independence testing via u -statistic permutation tests*, arXiv preprint arXiv:2001.05513, (2020).
- [8] D. M. BLEI, A. KUCUKELBIR, AND J. D. MCAULIFFE, *Variational inference: A review for statisticians*, Journal of the American Statistical Association, 112 (2017), pp. 859–877.
- [9] B. BROWN, K. ZHANG, AND X.-L. MENG, *BELIEF in dependence: Leveraging atomic linearity in data bits for rethinking generalized linear models*, The Annals of Statistics, 53 (2025), pp. 1068–1094.
- [10] S. CAO AND P. J. BICKEL, *Correlations with tailored extremal properties*, arXiv preprint arXiv:2008.10177, (2020).
- [11] S. CHATTERJEE, *A new coefficient of correlation*, Journal of the American Statistical Association, 116 (2021), pp. 2009–2022.
- [12] S. CHATTERJEE, *A survey of some recent developments in measures of association*, Probability and stochastic processes: a volume in Honour of Rajeeva L. Karandikar, (2024), pp. 109–128.
- [13] D. S. COLLINGRIDGE, *A primer on quantitized data analysis and permutation testing*, Journal of Mixed Methods Research, 7 (2013), pp. 81–97.
- [14] J. W. COOLEY AND J. W. TUKEY, *An algorithm for the machine calculation of complex Fourier series*, Mathematics of computation, 19 (1965), pp. 297–301.
- [15] L. DE HAAN, A. FERREIRA, AND A. FERREIRA, *Extreme value theory: an introduction*, vol. 21, Springer, 2006.
- [16] N. DEB, P. GHOSAL, AND B. SEN, *Measuring association on topological spaces using kernels and geometric graphs*, arXiv preprint arXiv:2010.01768, (2020).
- [17] N. DEB AND B. SEN, *Multivariate rank-based distribution-free nonparametric testing using measure transportation*, Journal of the American Statistical Association, 0 (2021), pp. 1–16, <https://doi.org/10.1080/01621459.2021.1923508>.
- [18] N. DEBROY, N. P. PITSIANIS, AND X. SUN, *Accelerating nonuniform fast Fourier transform via reduction in memory access latency*, in Advanced Signal Processing Algorithms, Architectures, and Implementations XVIII, vol. 7074, International Society for Optics and Photonics, 2008, p. 707404.
- [19] A. DUTT AND V. ROKHLIN, *Fast Fourier transforms for nonequispaced data*, SIAM Journal on Scientific computing, 14 (1993), pp. 1368–1393.
- [20] E. EDGINGTON AND P. ONGHENA, *Randomization tests*, CRC press, 2007.
- [21] R. A. FISHER, *Design of experiments*, British Medical Journal, 1 (1936), p. 554.
- [22] J. H. FRIEDMAN AND N. I. FISHER, *Bump hunting in high-dimensional data*, Statistics and Computing, 9 (1999), pp. 123–143.
- [23] J. H. FRIEDMAN AND W. STUETZLE, *Projection pursuit regression*, Journal of the American statistical Association, 76 (1981), pp. 817–823.
- [24] K. FUKUMIZU, F. R. BACH, AND M. I. JORDAN, *Kernel dimension reduction in regression*, The Annals of Statistics, 37 (2009), pp. 1871 – 1905, <https://doi.org/10.1214/08-AOS637>.
- [25] G. GEENENS AND P. LAFAYE DE MICHEAUX, *The Hellinger correlation*, Journal of the American Statistical Association, 117 (2022), pp. 639–653.
- [26] C. GENEST, J. NEŠLEHOVÁ, B. RÉMILLARD, AND O. MURPHY, *Testing for independence in arbitrary distributions*, Biometrika, 106 (2019), pp. 47–68.
- [27] C. GENEST AND F. VERRET, *Locally most powerful rank tests of independence for copula models*, Non-parametric Statistics, 17 (2005), pp. 521–539.
- [28] L. GREENGARD AND J.-Y. LEE, *Accelerating the nonuniform fast Fourier transform*, SIAM review, 46 (2004), pp. 443–454.
- [29] A. GRETTON, K. FUKUMIZU, C. H. TEO, L. SONG, B. SCHÖLKOPF, AND A. J. SMOLA, *A kernel statistical test of independence*, in Advances in neural information processing systems, 2007, pp. 585–592.
- [30] A. HAAR, *Zur theorie der orthogonalen funktionensysteme*, Mathematische Annalen, 69 (1910), pp. 331–371.
- [31] T. J. HASTIE, *Generalized additive models*, in Statistical models in S, Routledge, 2017, pp. 249–307.

- [32] M. HEIDEMAN, D. JOHNSON, AND C. BURRUS, *Gauss and the history of the fast Fourier transform*, IEEE ASSP Magazine, 1 (1984), pp. 14–21.
- [33] R. HELLER AND Y. HELLER, *Multivariate tests of association based on univariate tests*, in Advances in Neural Information Processing Systems 29, D. D. Lee, M. Sugiyama, U. V. Luxburg, I. Guyon, and R. Garnett, eds., Curran Associates, Inc., 2016, pp. 208–216, <http://papers.nips.cc/paper/6220-multivariate-tests-of-association-based-on-univariate-tests.pdf>.
- [34] R. HELLER, Y. HELLER, AND M. GORFINE, *A consistent multivariate test of association based on ranks of distances*, Biometrika, 100 (2013), pp. 503–510.
- [35] R. HELLER, Y. HELLER, S. KAUFMAN, B. BRILL, AND M. GORFINE, *Consistent distribution-free k -sample and independence tests for univariate random variables*, Journal of Machine Learning Research, 17 (2016), pp. 1–54.
- [36] Z. JIN AND D. MATTESON, *Generalizing distance covariance to measure and test multivariate mutual dependence via complete and incomplete v -statistics*, Journal of Multivariate Analysis, 168 (2018), pp. 304–322.
- [37] J. KINNEY AND G. ATWAL, *Equitability, mutual information, and the maximal information coefficient*, Proceedings of the National Academy of Sciences, 111 (2014), pp. 3354–3359.
- [38] I. KOJADINOVIC AND M. HOLMES, *Tests of independence among continuous random vectors based on Cramér–von Mises functionals of the empirical copula process*, Journal of Multivariate Analysis, 100 (2009), pp. 1137–1154.
- [39] D. LEE, K. ZHANG, AND M. R. KOSOROK, *Testing independence with the binary expansion randomized ensemble test*, arXiv preprint arXiv:1912.03662, (2019).
- [40] J.-Y. LEE AND L. GREENGARD, *The type 3 nonuniform FFT and its applications*, Journal of Computational Physics, 206 (2005), pp. 1–5.
- [41] K.-C. LI, *Sliced inverse regression for dimension reduction*, Journal of the American Statistical Association, 86 (1991), pp. 316–327.
- [42] D. W. LOZIER, *NIST digital library of mathematical functions*, Annals of Mathematics and Artificial Intelligence, 38 (2003), pp. 105–119.
- [43] L. MA AND J. MAO, *Fisher exact scanning for dependency*, Journal of the American Statistical Association, 114 (2019), pp. 245–258.
- [44] M. L. MEHTA, *Random matrices*, Elsevier, 2004.
- [45] G. MICHAELIDIS AND S. STOEY, *Extreme value theory: an introduction*, 2007.
- [46] N. PFISTER, P. BÜHLMANN, B. SCHÖLKOPF, AND J. PETERS, *Kernel-based tests for joint independence*, Journal of the Royal Statistical Society Series B: Statistical Methodology, 80 (2018), pp. 5–31.
- [47] D. POTTS, G. STEIDL, AND M. TASCHE, *Fast Fourier transforms for nonequispaced data: A tutorial*, Modern sampling theory, (2001), pp. 247–270.
- [48] D. N. RESHEF, Y. A. RESHEF, H. K. FINUCANE, S. R. GROSSMAN, G. MCVEAN, P. J. TURNBAUGH, E. S. LANDER, M. MITZENMACHER, AND P. C. SABETI, *Detecting novel associations in large data sets*, Science, 334 (2011), pp. 1518–1524.
- [49] D. N. RESHEF, Y. A. RESHEF, P. C. SABETI, AND M. M. MITZENMACHER, *An empirical study of leading measures of dependence*, arXiv preprint arXiv:1505.02214, (2015).
- [50] Y. A. RESHEF, D. N. RESHEF, P. C. SABETI, AND M. M. MITZENMACHER, *Equitability, interval estimation, and statistical power*, arXiv preprint arXiv:1505.02212, (2015).
- [51] M. ROSENBLATT, *Remarks on some nonparametric estimates of a density function*, The annals of mathematical statistics, (1956), pp. 832–837.
- [52] D. SEJIDINOVIC, B. SRIPERUMBUDUR, A. GRETTON, AND K. FUKUMIZU, *Equivalence of distance-based and RKHS-based statistics in hypothesis testing*, The Annals of Statistics, 10 (2014), pp. 2263–2291.
- [53] H. SHI, M. HALLIN, M. DRTON, AND F. HAN, *Rate-optimality of consistent distribution-free tests of independence based on center-outward ranks and signs*, arXiv preprint arXiv:2007.02186, (2020).
- [54] E. J. STOLLNITZ, A. DEROSE, AND D. H. SALESIN, *Wavelets for computer graphics: a primer. 1*, IEEE computer graphics and applications, 15 (1995), pp. 76–84.
- [55] G. STRANG, *Wavelet transforms versus Fourier transforms*, Bulletin of the American Mathematical Society, 28 (1993), pp. 288–305.
- [56] G. J. SZÉKELY, M. L. RIZZO, AND N. K. BAKIROV, *Measuring and testing dependence by correlation of distances*, The Annals of Statistics, 35 (2007), pp. 2769–2794, <https://doi.org/10.1214/>

009053607000000505.

- [57] T. TAO, *Topics in random matrix theory*, vol. 132, American Mathematical Soc., 2012.
- [58] A. R. THOMPSON, J. M. MORAN, AND G. W. SWENSON, *Interferometry and synthesis in radio astronomy*, Springer Nature, 2017.
- [59] C. A. TRACY AND H. WIDOM, *Distribution functions for largest eigenvalues and their applications*, arXiv preprint math-ph/0210034, (2002).
- [60] J. L. WALSH, *A closed set of normal orthogonal functions*, American Journal of Mathematics, 45 (1923), pp. 5–24.
- [61] E. W. WEISSTEIN, *Extreme value distribution*, From MathWorld—A Wolfram Web Resource. <https://mathworld.wolfram.com/ExtremeValueDistribution.html>, (2021).
- [62] Y. XIA, H. TONG, W. K. LI, AND L.-X. ZHU, *An adaptive estimation of dimension reduction space*, Journal of the Royal Statistical Society: Series B (Statistical Methodology), 64 (2002), pp. 363–410.
- [63] K. ZHANG, *BET on independence*, Journal of the American Statistical Association, 114 (2019), pp. 1620–1637, <https://doi.org/10.1080/01621459.2018.1537921>.
- [64] K. ZHANG, Z. ZHAO, AND W. ZHOU, *BEAUTY powered BEAST*, arXiv preprint arXiv:2103.00674, (2021).
- [65] S. ZHENG, N.-Z. SHI, AND Z. ZHANG, *Generalized measures of correlation for asymmetry, nonlinearity, and beyond*, Journal of the American Statistical Association, 107 (2012), pp. 1239–1252.
- [66] L. ZHU, K. XU, R. LI, AND W. ZHONG, *Projection correlation between two random vectors*, Biometrika, 104 (2017), pp. 829–843.